

Tunable generation of Bessel beams with a fluidic axicon

Graham Milne, Gavin D. M. Jeffries, and Daniel T. Chiu^{a)}

Department of Chemistry, University of Washington, Seattle, Washington 98195-1700, USA

(Received 20 March 2008; accepted 9 June 2008; published online 30 June 2008)

This paper describes a tunable fluidic conical lens, or axicon, for the generation and dynamic reconfiguration of Bessel beams. When illuminated with a Gaussian laser beam, our fluidic axicon generates a diverging beam with an annular cross section. By varying the refractive index of the solution that fills our device, we can vary easily the spatial properties of the resulting Bessel beam. © 2008 American Institute of Physics. [DOI: 10.1063/1.2952833]

Bessel beams have received much attention in recent years, owing to their interesting optical properties (for a recent review, see Ref. 1). The propagation-invariant properties of the core of the beam, for example, have led to applications in atom optics,² the formation of one-dimensional colloidal structures,³ and the guiding of aerosol droplets.⁴ Because the wavevectors that interfere to produce the Bessel beam can be thought of as lying on a cone, the bright core of the Bessel beam has the ability to reform after an obstacle. In the context of optical trapping, this property has been exploited to manipulate simultaneously particles in multiple planes.⁵ Recently, the propagation-invariant and self-healing properties of Bessel beams have been used to enable efficient two-photon photoporation and transfection of cells,⁶ avoiding the need for the careful positioning of a small focal region. In addition, the concentric rings of light associated with the transverse intensity profile have been used to enable the static optical sorting of both silica microspheres, as a function of size⁷ and human blood cells, as a function of shape.⁸ Experimentally, Bessel beams can be generated through the illumination of an axicon with a monochromatic plane wave.⁹ An axicon can be thought of as a cone-shaped prism and is typically characterized by the angle γ , as defined in Fig. 1(a). Bessel beams were first proposed by Durnin in 1987 as propagation-invariant solutions to the Helmholtz equation.¹⁰ The Bessel beam gets its name from its radial transverse intensity profile, $I(r, z)$, which can be described theoretically in terms of Bessel functions [Eq. (1)]. In practice, experimental Bessel beams are at best approximations to Durnin's ideal case. Nevertheless, the beams produced by axicons retain many of the interesting properties highlighted in Durnin's original work. While high-order Bessel beams are experimentally possible,¹¹ for this work, we consider only the zeroth-order case:

$$I(r, z) = \frac{4k_r P}{w_c z_{\max}} \frac{z}{z_{\max}} J_0^2(k_r r) \exp\left\{-\frac{2z^2}{z_{\max}^2}\right\}, \quad (1)$$

where J_0 is the zeroth-order Bessel function of the first kind, z is the displacement along the direction of propagation, P is the power of the incident beam, and w_c is the beamwaist of the beam illuminating the axicon. $k_r = k \sin \alpha$, where k is the wavenumber of the incident beam. α describes the angle subtended by the imaginary cone on which the wavevectors of the subsequent plane waves that interfere to form the Bessel

beam can be thought to lie. α is related to the opening angle of the axicon, γ , through the relationship

$$\alpha = (n_{\text{ax}} - 1)\gamma, \quad (2)$$

where n_{ax} is the refractive index of the axicon. Figure 1(a) shows the form of a typical zeroth-order Bessel beam produced using a conventional axicon. The cross-sectional profile [Fig. 1(b)] consists of a bright core surrounded by concentric rings of decreasing radial intensity. For this work, the illuminating beamwaist was set to $w_c = 1$ mm. Figure 1(b) (inset) shows the profile of an experimental beam produced by a conventional 1° axicon. The parameters of interest for applications using Bessel beams are the propagation distance, z_{\max} , the typical ring spacing, $\Delta\rho$, and the size of the beam core, r_0 , defined as the radial distance from the core to the first intensity minimum. These terms are given by the following expressions:

$$z_{\max} = w_c / (\tan \alpha), \quad (3)$$

$$\Delta\rho \approx \lambda / (2 \sin \alpha), \quad (4)$$

$$r_0 = 2.405 / (k \sin \alpha). \quad (5)$$

In Eq. (5), the factor of 2.405 is derived from the first root of the zeroth-order Bessel function. In all three cases, the parameters of interest are a function of γ , from Eq. (2). To gain true control over the functionality of these systems, therefore, it is necessary to be able to vary the effective cone angle of the axicon. Axicons are expensive specialized optics and are usually manufactured from solid materials such as BK7 glass or fused silica. Varying the effective cone angle is not a straightforward task. Nevertheless, various schemes have been proposed and implemented due to the importance of gaining this degree of control.

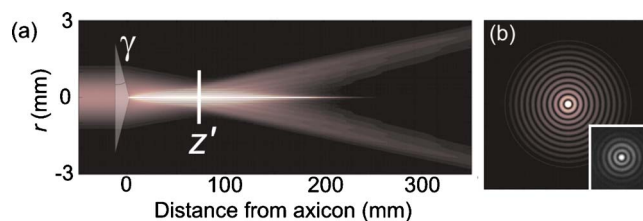


FIG. 1. (Color online) (a) When illuminated with a coaxial Gaussian beam, an axicon produces a characteristic interference pattern, known as a Bessel beam. (b) Theoretical cross-sectional profile taken at z' in (a). (Inset) Experimental Bessel beam generated by a $\gamma = 1^\circ$ axicon.

^{a)}Electronic mail: chiu@chem.washington.edu.

The effective cone angle can be altered by adding a telescope after the axicon. Vaicaitis *et al.*¹² have suggested that the effective cone angle can be varied by moving the axicon between two fixed lenses. Unfortunately, the generation of an azimuthally symmetric Bessel beam is extremely sensitive to misalignment in the optical train, and the physical movement of optical components is arguably best avoided. Spatial light modulators (SLMs), which are dynamically reconfigurable, have been used to generate Bessel beams.^{13,14} The kinoforms displayed on the SLM provide a phase transformation equivalent to the passage of the beam through an axicon. The algorithm for their calculation is straightforward and can be varied in real time. SLMs, however, introduce their own set of drawbacks. SLMs are very expensive and are prone to aberrations introduced in the manufacturing process, although the impact of these aberrations can be reduced through the addition of corrective terms to the kinoform. For effective cone angles greater than several milliradians, the fidelity of the Bessel beam can be undermined by aliasing, due to the finite pixel resolution of the device. Additionally, a blazing function must often be employed to displace the Bessel beam from the undiffracted zeroth-order spot. As a result, a significant proportion of light is lost by the SLM when compared to a conventional axicon. Generally, due to the potential damage caused by heating, liquid crystal-based SLMs place a strict limit on the power of the illuminating beam, which can be an important constraint for applications that require high laser powers. Finally, the small size of many commercial SLMs limits the maximum possible propagation distance z_{\max} . Another recent alternative has been proposed by Macleod *et al.*¹⁵ using a tunable acoustic gradient lens. The authors note that the beam produced by this approach has a transversal profile that varies somewhat from that produced by an axicon, which may make it unsuitable for some applications. To address these issues, this paper presents a new method for fabricating an axicon with an effective cone angle that can be tuned over a continuous range while avoiding some of the pitfalls associated with the alternative approaches described above.

The construction of our fluidic axicon was an extremely simple process. We used a commercially available glass axicon (EKSPLA, Lithuania, $\gamma=5^\circ$) as a template. This axicon was submerged in polydimethylsiloxane (PDMS) and cured. The glass axicon was then removed, leaving a cone-shaped cavity inside the PDMS block. The block was sealed between two glass microscope slides, ensuring flat and parallel optical surfaces. Small inlet and outlet channels were inserted through the PDMS to enable the filling of the conical cavity with liquid of known refractive index. Figure 2(a) shows a photograph of the completed fluidic axicon. Although we chose PDMS for the inverse molding of the axicon, any polymer that has high replication fidelity and the appropriate optical properties can be used. Our fluidic axicon was illuminated with a collimated, linearly polarized 1064 nm Gaussian beam, produced by a Millennia IR laser (Spectra Physics, Mountain View, CA). Images of the resultant Bessel beam were captured directly using a Prosilica GC660 charge coupled device camera. If a fluid with a higher refractive index than PDMS is used, a Bessel beam forms immediately after the fluidic axicon [Fig. 2(b)]. When the refractive index of the fluidic medium (e.g., water with $n=1.33$) filling the cavity is lower than that of PDMS ($n \approx 1.43$), it is necessary to include a telescope after the axicon

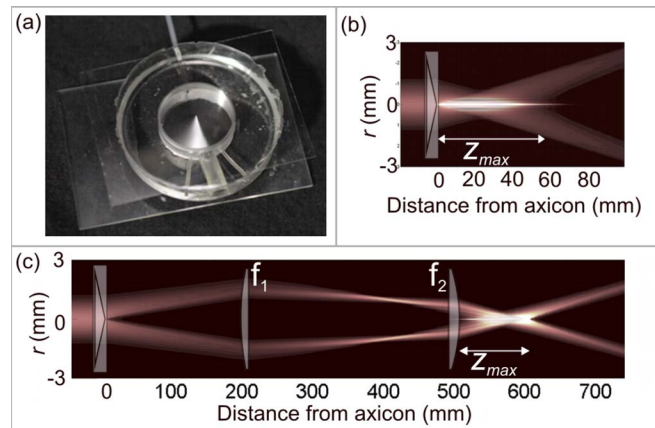


FIG. 2. (Color online) (a) Photograph of our fluidic axicon prototype. (b) Fluidic axicon with $n_{\text{ax}} > n_{\text{PDMS}}$. (c) Fluidic axicon with $n_{\text{ax}} < n_{\text{PDMS}}$. z_{\max} indicates the approximate propagation distance of the beam core in each case.

to form the Bessel beam; Fig. 2(c) illustrates this geometry. We chose to use a range of water-based sucrose solutions with refractive indices lower than that of PDMS.

A straightforward geometrical analysis suggests that the imaginary cone on which the wavevectors of the beam formed by our fluidic axicon lie can be described by the equation

$$\alpha_1 = \sin^{-1} \left(\frac{n_{\text{PDMS}}}{n_{\text{air}}} \sin \left(\sin^{-1} \left(\frac{n_{\text{ax}}}{n_{\text{PDMS}}} \sin \gamma \right) - \gamma \right) \right). \quad (6)$$

This expression can be simplified by assuming $n_{\text{air}} \approx 1$ and $\sin \gamma \approx \gamma$, which is appropriate when considering the small opening angles normally associated with axicons. With these modifications, Eq. (6) simplifies to

$$\alpha_1 = (n_{\text{ax}} - n_{\text{PDMS}}) \gamma. \quad (7)$$

This closely matches the form of the equivalent expression for a conventional axicon, as given in Eq. (2). When using the geometry shown in Fig. 2(c), the effective cone angle associated with the resultant Bessel beam is given by $\alpha_2 = -(f_1/f_2)\alpha_1$. To verify experimentally our fluidic axicon's tunability, we measured the beam core size (defined as the distance from the center of the beam to the first radial intensity minimum) for a number of different sucrose concentrations. Of the three characteristic parameters of a Bessel beam described above [Eqs. (3)–(5)], the beam core size is the easiest to measure accurately. Figure 3(a) shows some recorded profiles and Fig. 3(b) plots measurements of the beam core size as a function of the refractive index of the solution. The experimental results show an almost linear increase in beam size with refractive index. Superimposed on the plot are theoretical calculations for the beam width. The theoretical beam width is given by Eq. (5), and from Eq. (7) we can see that α will tend to zero as $n_{\text{ax}} \rightarrow n_{\text{PDMS}}$. Because of this, the theoretical curve for the beam core width is asymptotic at $n_{\text{ax}} = n_{\text{PDMS}}$. In reality, we see that when the refractive indices are closely matched, the device has little effect and we recover a Gaussian beam.

While refilling our device does not noticeably affect beam alignment, we note that our design introduces a settling time due to the turbulence generated whenever a new solution is injected to the chamber. This settling time is a function of the size of the chamber and the viscosity of the solu-

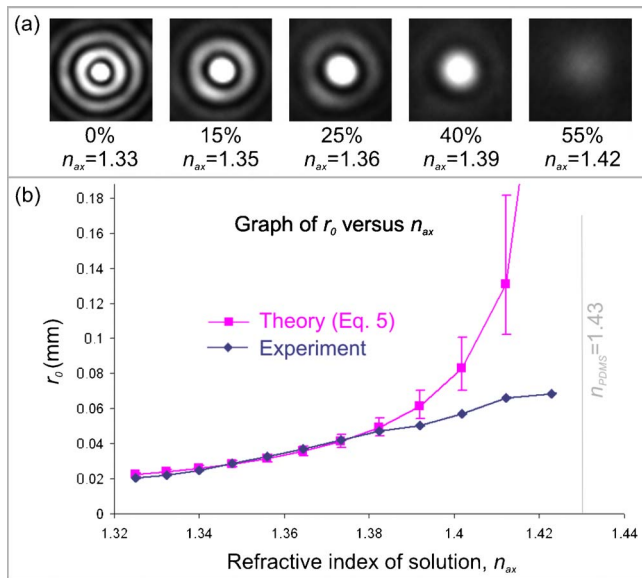


FIG. 3. (Color online) (a) Bessel beam cross sections, taken 5 cm after lens f_2 , for a range of sucrose concentrations. In the last case (55%, $n_{ax} \approx n_{PDMS}$), the axicon's effect is negligible and we recover a Gaussian beam profile. (b) A plot of the measured Bessel beam core widths against the refractive indices of the fluidic medium in the axicon cavity. For our theoretical calculations, we assumed $n_{PDMS} = 1.43 \pm .005$. The theoretical curve is asymptotic as $n_{ax} \rightarrow n_{PDMS}$, but in reality at this point the beam reverts back to a Gaussian beam and the concept of the Bessel beam core becomes redundant.

tion that has been injected, and is of the order of 10 s in our experiments, which may limit our device for high-speed applications. With better fluidic input-output design to minimize turbulence, coupled with fast fluidic switching techniques, it should be possible to reduce greatly this settling time. We also note that PDMS is elastomeric, and as such, the experimentally measured beam size can differ from the calculated one by a small constant scaling factor, which accounts for any slight flexing of the flat face of the axicon. Practically, this should not pose any inconveniences as the axicon is tunable; the use of a rigid material should minimize this effect we see with PDMS. Although we used a fluidic medium with a refractive index lower than that of the PDMS substrate, we note that high refractive index fluids (e.g., silicone oils) could also be employed.

In summary, fluidic axicons offer a simple and cost-effective solution for the tunable generation of Bessel beams. Unlike SLMs, fluidic axicons can cope with high laser powers and are, in principle, completely scalable. Another key advantage is that through the use of a fluidic approach, we avoid alignment issues associated with the need to physically displace optical components. For ease of implementation, we used PDMS as the substrate of our fluidic axicon. To extend the tunable range of the axicon, other materials with a higher refractive index, including glass or other optically transparent polymers, could be used. Replica molding offers a simple route to manufacture fluidic axicons, but a number of other replication methods, such as injection molding and embossing, may also be employed. The ease with which the parameters of the Bessel beam can be controlled through the use of a fluidic axicon should further facilitate the study of this interesting optical beam and expand its applications.

The authors gratefully acknowledge NIH (EB005197) for support of this work.

- ¹D. McGloin and K. Dholakia, *Contemp. Phys.* **46**, 15 (2005).
- ²J. Arlt, T. Hitomi, and K. Dholakia, *Appl. Phys. B: Lasers Opt.* **71**, 549 (2000).
- ³V. Garces-Chavez, D. McGloin, M. Summers, A. Fernandez-Nieves, G. Spalding, G. Crisobal, and K. Dholakia, *J. Opt. A, Pure Appl. Opt.* **6**, S235 (2004).
- ⁴M. Summers, J. Reid, and D. McGloin, *Opt. Express* **14**, 6373 (2006).
- ⁵V. Garces-Chavez, D. McGloin, H. Melville, W. Sibbett, and K. Dholakia, *Nature (London)* **419**, 145 (2002).
- ⁶X. Tsampoula, V. Garces-Chavez, M. Comrie, D. Stevenson, M. Agate, F. Gunn-Moore, C. Brown, and K. Dholakia, *Appl. Phys. Lett.* **91**, 053902 (2007).
- ⁷G. Milne, K. Dholakia, D. McGloin, K. Volke-Sepulveda, and P. Zemnek, *Opt. Express* **15**, 13972 (2007).
- ⁸L. Paterson, E. Papagiakoumou, G. Milne, V. Garces-Chavez, S. A. Tatarkova, W. Sibbett, F. Gunn-Moore, P. Bryant, A. Riches, and K. Dholakia, *Appl. Phys. Lett.* **87**, 123901 (2005).
- ⁹R. Herman and T. Wiggins, *J. Opt. Soc. Am. A* **8**, 932 (1991).
- ¹⁰J. Durnin, *J. Opt. Soc. Am. A* **4**, 651 (1987).
- ¹¹J. Arlt and K. Dholakia, *Opt. Commun.* **177**, 297 (2000).
- ¹²V. Vaicaitis and S. Paulikas, *Opt. Quantum Electron.* **35**, 1065 (2003).
- ¹³J. Davis, E. Carcole, and D. Cottrell, *Appl. Opt.* **35**, 2159 (1996).
- ¹⁴N. Chattaripiban, E. Rogers, D. Cofield, W. Hill, and R. Roy, *Opt. Lett.* **28**, 2183 (2003).
- ¹⁵E. McLeod, A. Hopkins, and C. Arnold, *Opt. Lett.* **31**, 3155 (2006).